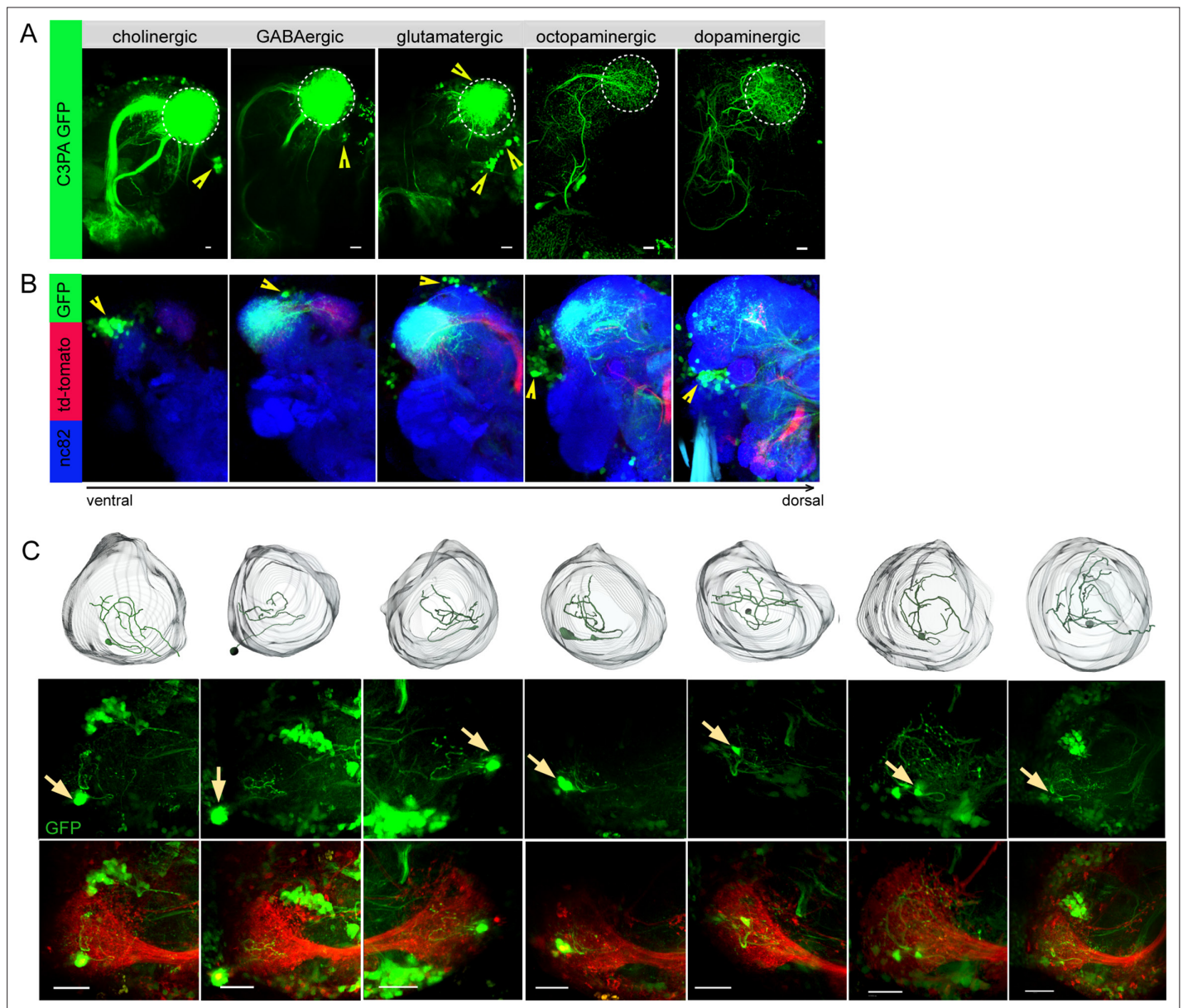# Figures and figure supplements

Higher-order olfactory neurons in the lateral horn support odor valence and odor identity coding in *Drosophila*

Sudeshna Das Chakraborty *et al*

Figure 1. Selective labeling of lateral horn neurons (LHNs) based on their neurotransmitter identities. (**A**) Photoactivation of *UAS-C3PA-GFP* expressed under the control of different Gal4 lines with various neurotransmitter and neuromodulator identities (*Cha-Gal4, GAD1-Gal4, dVGlut-Gal4, tdc2-Gal4,* and *TH-Gal4*) reveals subsets of cholinergic, GABAergic, glutamatergic, octopaminergic, and dopaminergic LHNs (left to right). Position of cell bodies is demarcated with yellow arrowheads. (**B**) Immunohistochemistry of photoactivated brains with *dVGlut-Gal4* driving *UAS-C3PA-GFP* reveals different cell body clusters of glutamatergic LHNs found at various locations in different focal planes. *GH146-QF* driving *QUAS-mtd tomato* in the background is depicted in red and nc82 in blue. Position of the cell bodies is shown with yellow arrowheads. (**C**) Single-neuron photoactivation of the dorsomedial cluster revealed individual glutamatergic LH local neurons (LHLNs). Upper panel shows the 3D reconstruction, middle and lower panels show the photoactivated neuron in the background of *GH146-QF, QUAS mtd Tomato*. Yellow arrow demarcates the position of the photoactivated cell body. Scale bars = 10 μm.
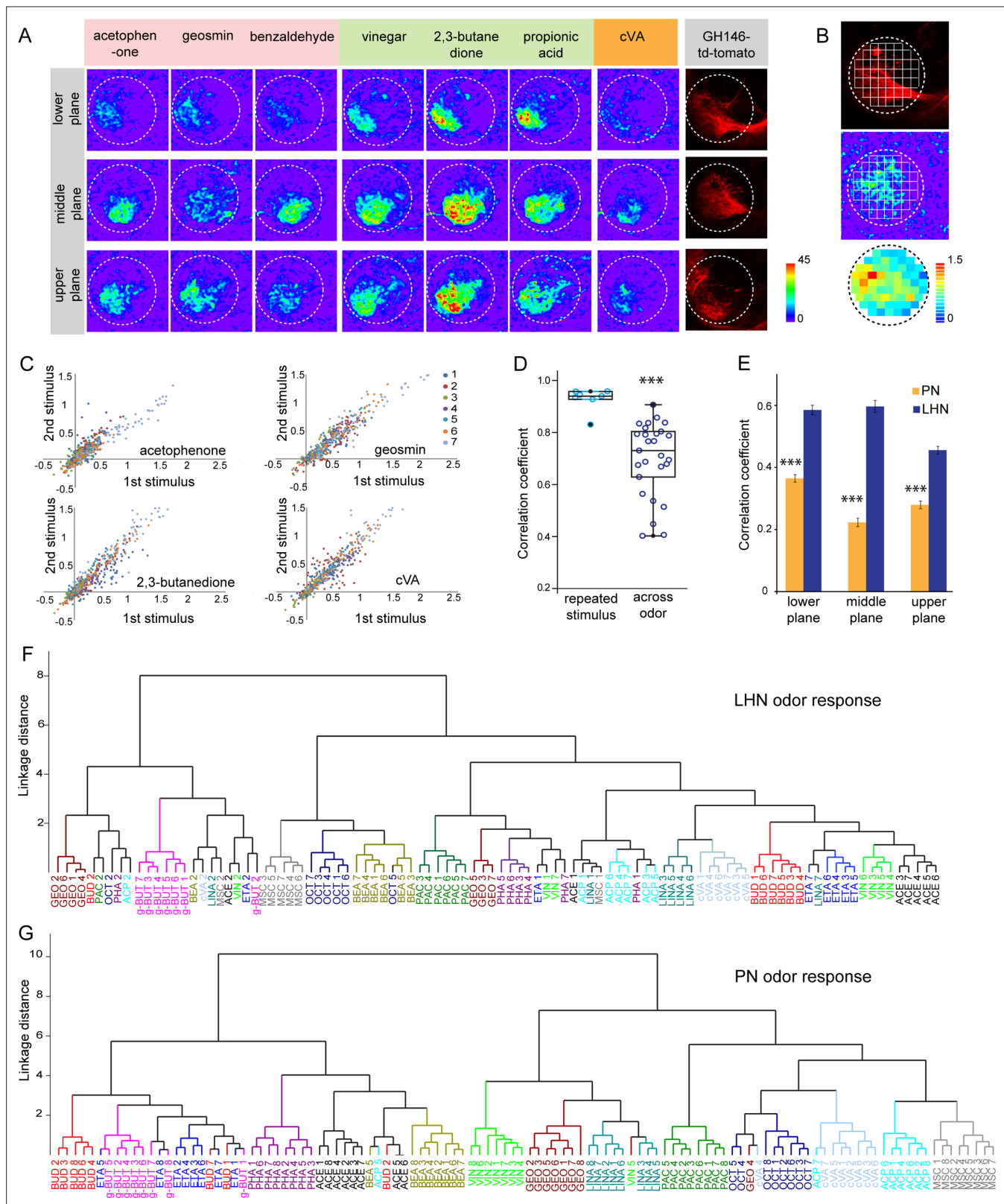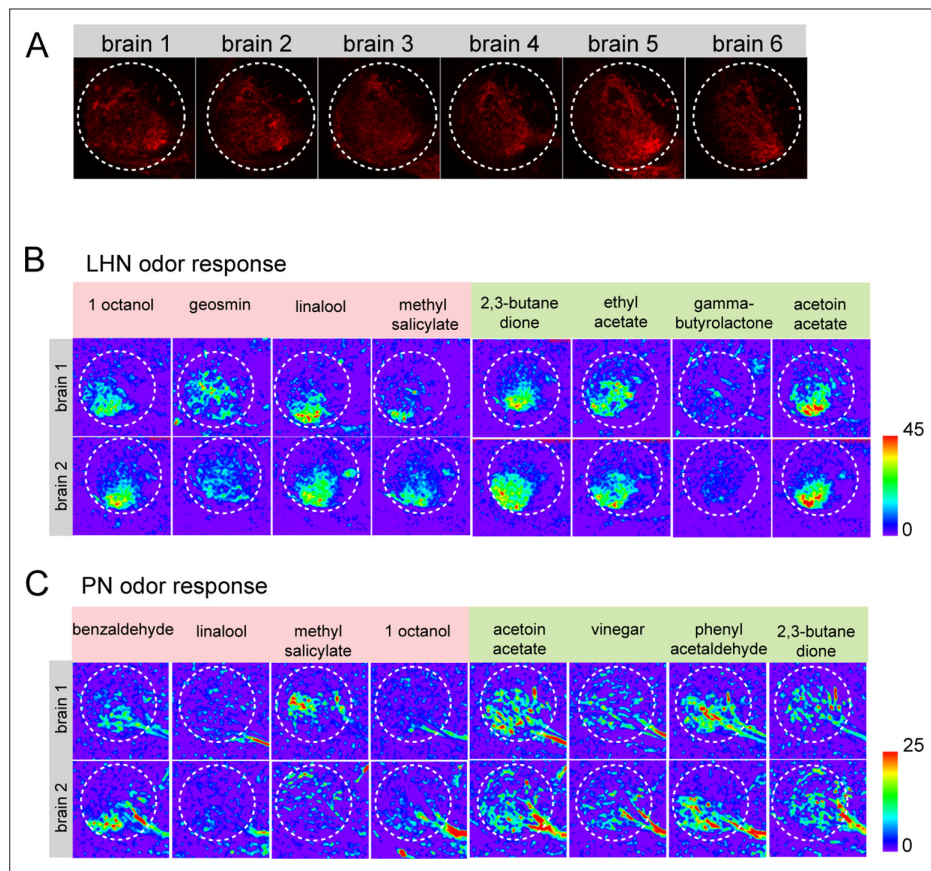
Figure 2. Odor response properties of glutamatergic lateral horn neurons (LHNs) and uniglomerular projection neurons (uPNs). (**A**) Representative images of calcium responses of glutamatergic LHNs in the LH brain area in three focal planes, evoked by various odors (repulsive odors: acetophenone, geosmin, benzaldehyde; attractive odors: vinegar, 2,3 butanedione, propionic acid; pheromone: cVA). Right panel shows the innervation pattern of uPNs labeled by GH146 in three different focal planes, used as a landmark to maintain comparable focal planes for functional imaging across

Figure 2 continued on next page

Figure 2 continued

different animals. (**B**) Grid approach to analyze odor-evoked responses of glutamatergic LHNs. Representative images of the grid onto uPN labeling (upper panel), used as a background landmark, odor-evoked responses of glutamatergic LHNs (middle panel) and analyzed ΔF/F of each pixels from glutamatergic LHNs in the LH area (lower panel). (**C**) Scatter plot showing calcium responses of each pixel of glutamatergic LHNs at middle plane to repeated presentation of an odor stimulus. Different colored dots depict responses obtained from different animals (n = 7). (**D**) Box plot represents comparison of odor-evoked responses of glutamatergic LHNs at middle plane, between repeated and across odor stimuli (Student's *t*-test, ***p<0.001). (**E**) Comparison of correlation coefficients of uPN and LHN responses at three different focal planes. Different odors seem to be better segregated at the uPN level than at the level of LHNs (Student's *t*-test, ***p<0.001). (**F**) Cluster analysis of LHN odor responses based on linkage distance (n = 7, ANOSIM, sequential Bonferroni significance, p=0.0001). (**G**) Cluster analysis of uPN odor responses based on linkage distance (n = 8; ANOSIM, sequential Bonferroni significance, p=0.0001). Both cluster analyses reveal that the majority of replicates for each odor are grouped together.

Figure 2—figure supplement 1. Stereotypy of *GH146-mtd Tomato* signal and the odor response pattern of lateral horn neurons (LHNs) and uniglomerular projection neurons (uPNs) across brains. (**A**) Representation of *GH146-QF, QUAS-mtd Tomato* at the middle plane across six brains reveals the signal stereotypy and the precise plane that has been used to measure glutamatergic LHN responses across flies. (**B**) Representative images of odor response patterns of glutamatergic LHNs of two flies to multiple odors demonstrating the spatial stereotypy of odor-evoked responses. (**C**) Representative images of odor response patterns of uPNs of two flies to multiple odors demonstrate the spatial stereotypy of the odor-evoked responses.
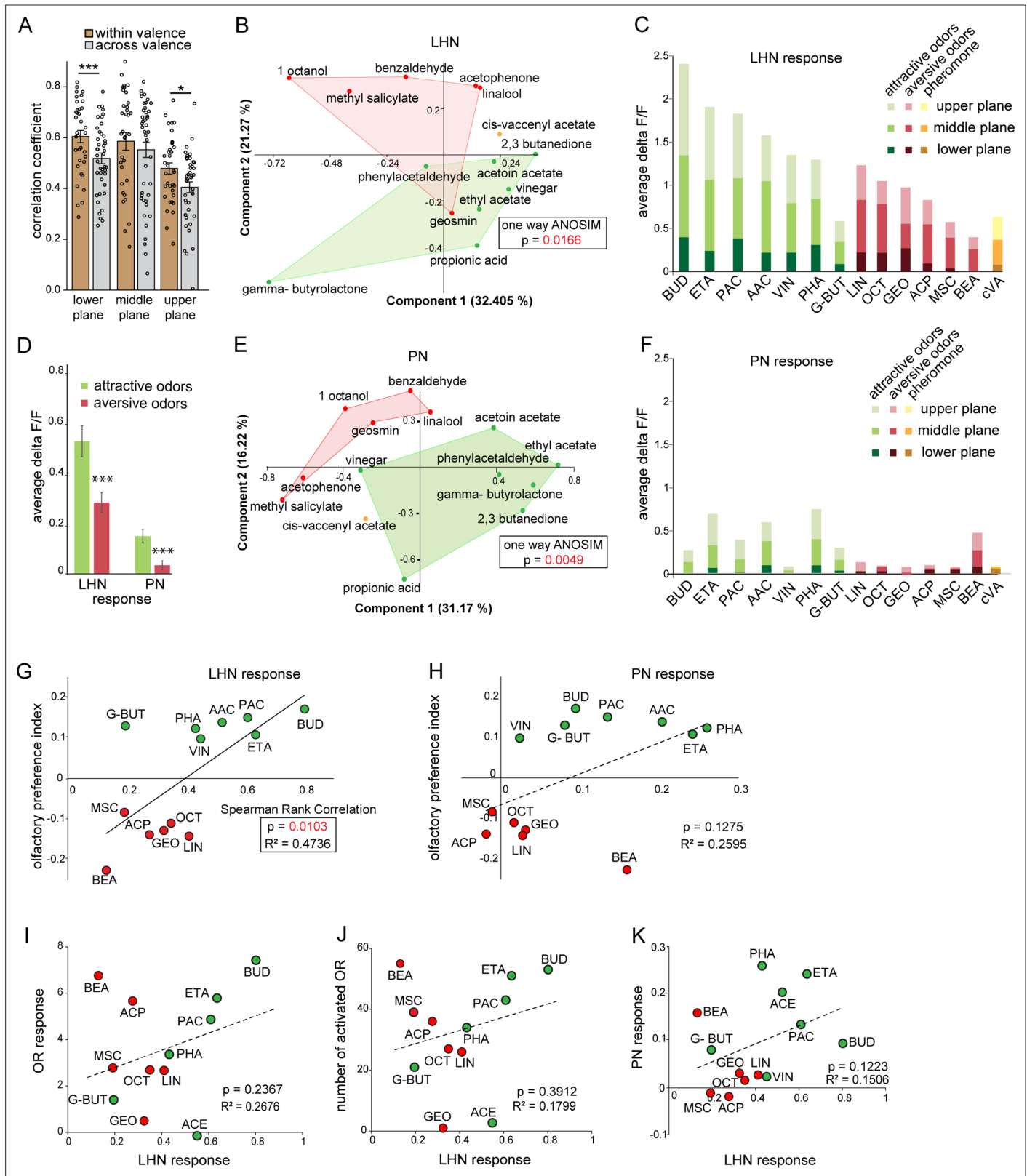
Figure 3. Segregation of hedonic valence in the lateral horn (LH). (**A**) Comparison of the correlation coefficients of odor responses of glutamatergic lateral horn neurons (LHNs) between the odors that share the same valence (i.e., within valence) and odors having an opposite valence (i.e., across valence). Responses to odors sharing the same valence are significantly more similar than those across valence (Student's *t*-test, ***p<0.001, *p<0.05). (**B**) Principal component analysis (PCA) of odor responses of glutamatergic LHNs shows that attractive (green) and aversive (red) odors are significantly

Figure 3 continued on next page

Figure 3 continued

segregated in the LH (one-way ANOSIM, p=0.0166). (**C**) Response amplitudes of glutamatergic LHNs to individual attractive and aversive odors. (**D**) Comparison of the overall response strength of glutamatergic LHNs and uniglomerular projection neurons (uPNs) to all attractive and aversive odors (Student's *t*-test, ***p<0.001). (**E**) PCA of odor responses of uPNs shows that attractive (green) and aversive (red) odors are significantly segregated in the LH (one-way ANOSIM, p=0.0049). (**F**) Response amplitudes of uPNs to individual attractive and aversive odors. (**G**) Scatter plot of olfactory preference indices of all tested odors to the response strengths of glutamatergic LHNs. The solid trend line demarcates significant correlation between the two parameters (Spearman rank correlation, p=0.01). (**H**) Scatter plot of olfactory preference indices of all tested odors to the response strengths of uPNs, which does not show a significant correlation (dotted trend line). (**I**) Scatter plot of the response strength of glutamatergic LHNs for individual odors to the overall olfactory sensory neuron (OSN) activity. (**J**) Scatter plot of the response strength of glutamatergic LHNs for individual odors to the number of ORs activated. (**K**) Scatter plot of the response strength of glutamatergic LHNs and the response strengths of uPNs for individual odors (for LHN recording n = 7 and for PN recording n = 8).
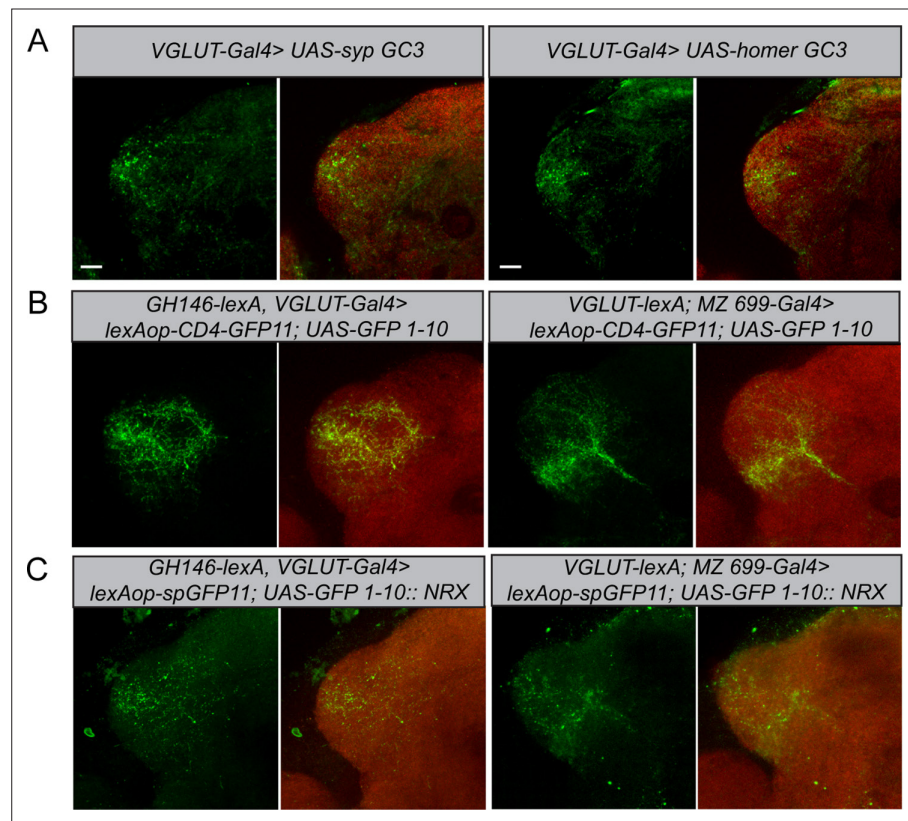
Figure 4. Polarity and morphological connectivity of glutamatergic lateral horn neurons (LHNs) with uniglomerular projection neurons (uPNs) and multiglomerular projection neurons (mPNs). (**A**) Expression of syp GC3 (left panel) and homer GC3 (right panel) in glutamatergic LHNs suggesting the presence of pre- as well as postsynapses in the LH. (**B**) Membrane-targeted CD4-GRASP between glutamatergic LHNs and uPNs (left panel) or mPNs (right panel). (**C**) The synaptic protein neurexin tagged to GRASP (*Nrx-GRASP*) was employed to confirm synaptic connectivity of glutamatergic LHNs with uPNs (left panel) or mPNs (right panel) in the LH. Scale bars = 10 μm.
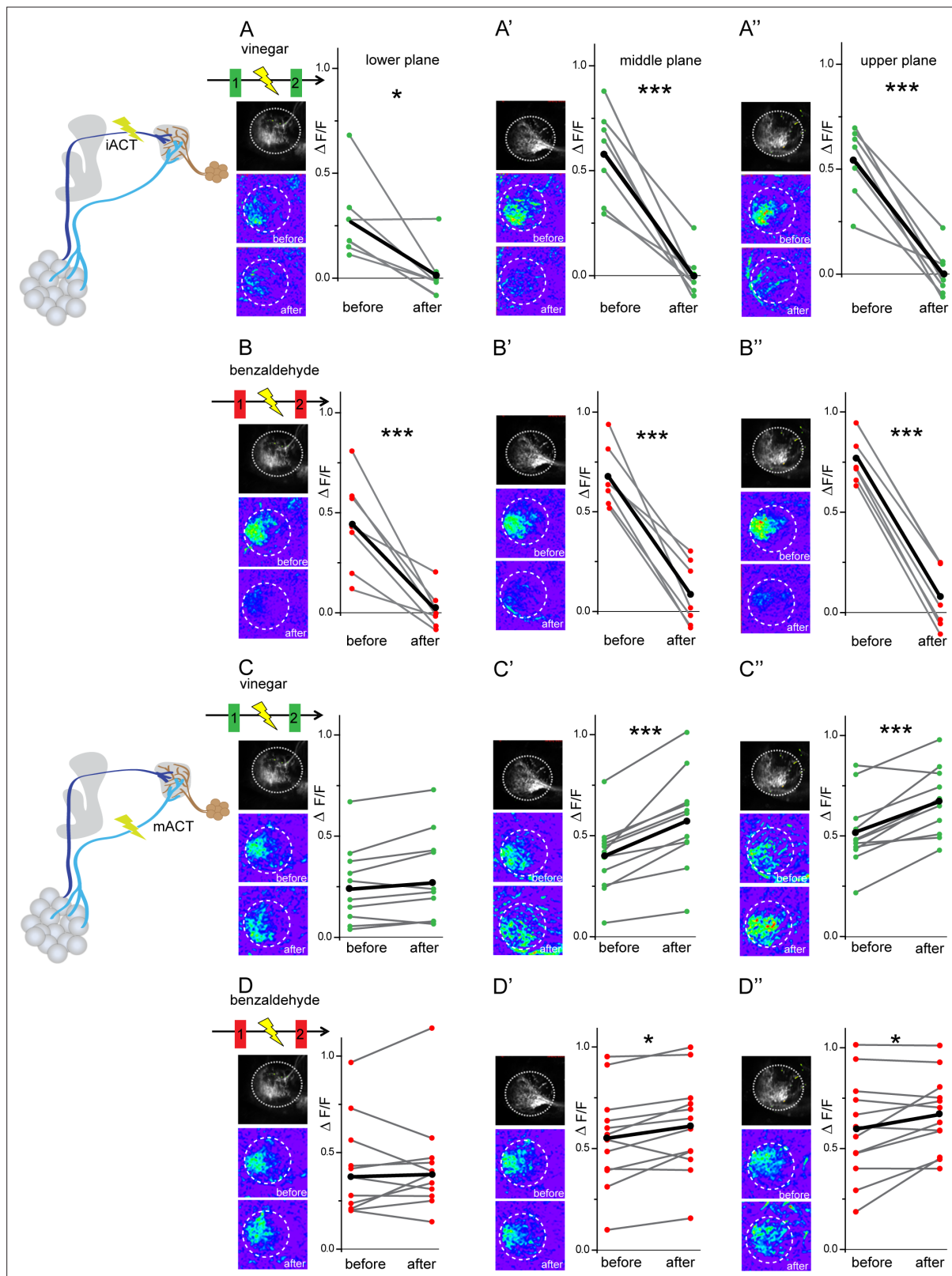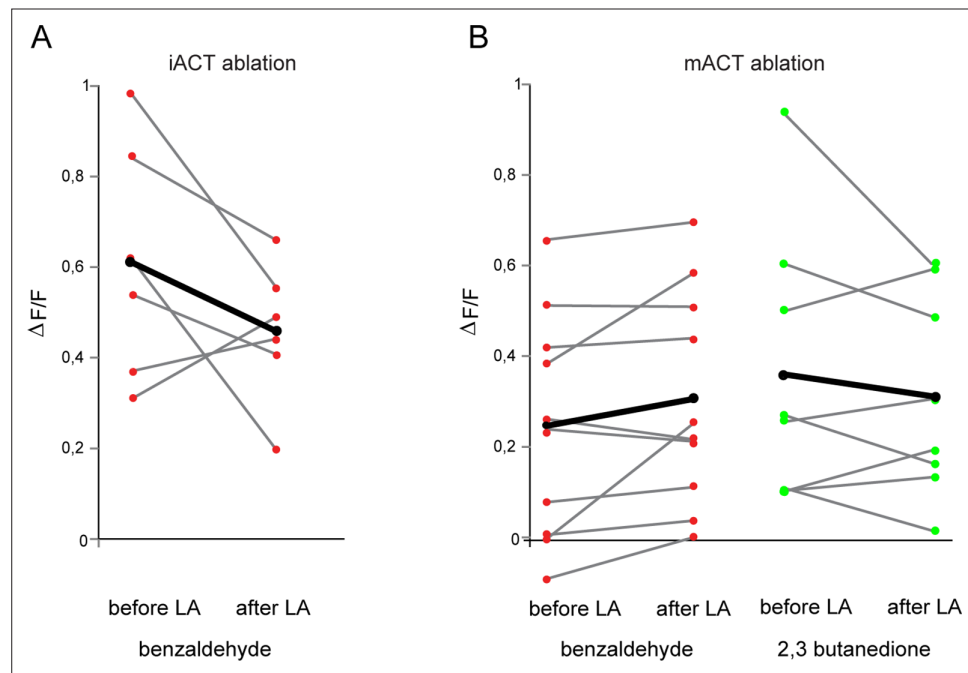
Figure 5. Glutamatergic lateral horn neurons (LHNs) receive their major excitatory input from uniglomerular projection neurons (uPNs) and an odorant-selective inhibition from multiglomerular projection neurons (mPNs). Upper panel schematic represents the experimental approach: the iACT tract was laser transected while odor-evoked responses were monitored from glutamatergic LHNs. (**A, A', A''**) Representative images and graphical comparison of responses evoked by vinegar in glutamatergic LHNs before and after laser transection of the iACT, across three different planes (n = 6). (**B, B',**

Figure 5 continued on next page

Figure 5 continued

B″) Representative images and graphical comparison of responses evoked by benzaldehyde in glutamatergic LHNs before and after laser transection of the iACT (n = 6). Lower panel schematic represents the experimental approach: the mACT tract was laser transected while odor-evoked responses were measured from glutamatergic LHNs. (**C, C′, C″**) Representative images and graphical comparison of vinegar-evoked responses of glutamatergic LHNs before and after laser transection of the mACT (n = 10). (**D, D′, D″**) Representative images and graphical comparison of benzaldehyde-evoked responses of glutamatergic LHNs before and after laser transection of the mACT (n = 10) (paired *t*-test ***p<0.001, *p<0.05). The red and green circles indicate individual data points for benzaldehyde and vinegar, respectively. The black circles indicate the averaged response.

Figure 5—figure supplement 1. Laser transaction does not affect activity of glutamatergic lateral horn neurons (LHNs) in the intact brain hemisphere. (**A**) Comparison of benzaldehyde-evoked activity in glutamatergic LHNs in the intact hemisphere, before and after laser ablation of the iACT in the other, treated brain hemisphere (n = 6) (paired *t*-test, p=0.19). (**B**) Comparison of benzaldehyde (n = 10) and 2,3 butanedione (n = 8)-evoked activities in glutamatergic LHNs in the intact hemisphere, before and after laser ablation of the mACT in the other hemisphere (paired *t*-test, p=0.084 for benzaldehyde and p=0.37 for 2,3 butanedione). The red and green circles indicate individual data points for benzaldehyde and 2,3 butanedione, respectively. The black circles indicate the averaged response.
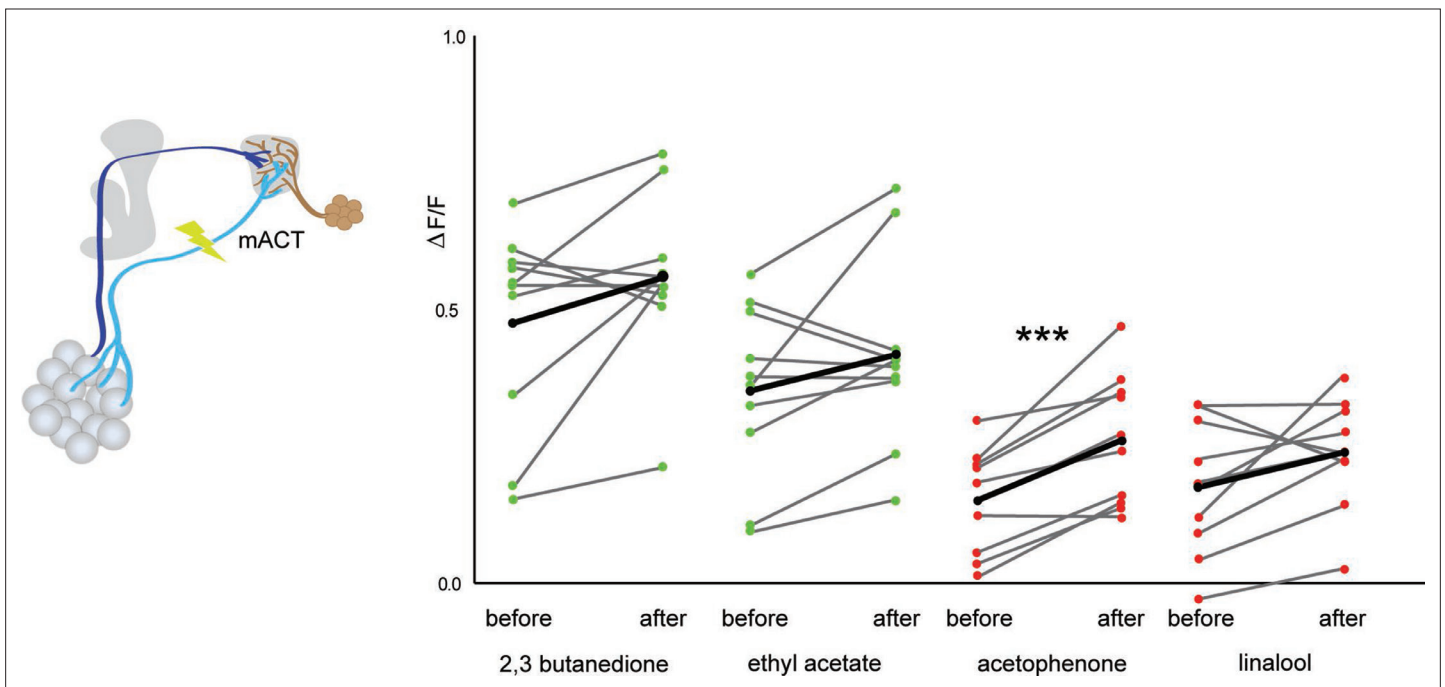
Figure 5—figure supplement 2. Multiglomerular projection neuron (mPN)-mediated odor-selective inhibition onto glutamatergic lateral horn neurons (LHNs). Comparison of glutamatergic LHN responses in the middle plane before and after laser transection of the mACT reveals a significant increase in activity only in the case of acetophenone (p=0.00059), whereas a trend was observed for other odors (2,3 butanedione [p=0.1], ethyl acetate [p=0.13], and linalool [0.083]) (paired *t*-test, n = 10). The red and green circles indicate individual data points for aversive odors (acetophenone and linalool) and attractive odors (2,3 butanedione and ethyl acetate), respectively. The black circles indicate the averaged response.
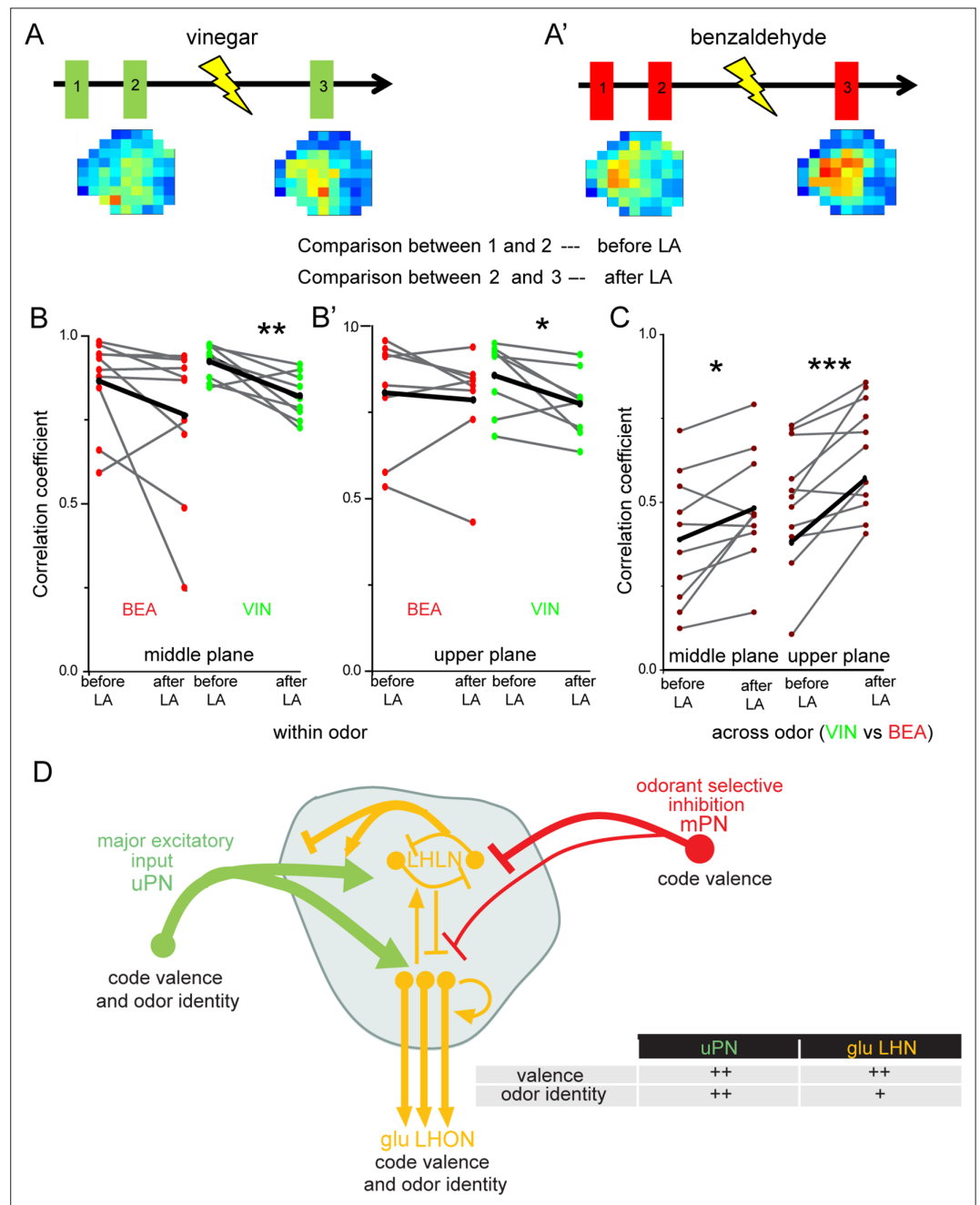
Figure 6. Multiglomerular projection neuron (mPN)-mediated inhibition facilitates odor specificity in glutamatergic lateral horn neurons (LHNs). (**A, A'**) Schematic representing the experimental approach: odor-evoked responses of glutamatergic LHNs were monitored to repeated odor presentations (1 and 2) before and after laser transection of the mACT (3) for the odors vinegar and benzaldehyde. (**B, B'**) Comparison of the correlation coefficients between repeated odor responses before laser ablation to those after the transection for vinegar and benzaldehyde (within odor comparison) (n = 7–9). (**C**) Comparison of the correlation coefficients across vinegar and benzaldehyde before and after microlesion (across odor comparison; paired *t*-test, ***p<0.001, **p<0.005, *p<0.05) (n = 10–11). (**D**) Schematic summarizing the observed connectivity between PNs and glutamatergic LHNs in the LH: glutamatergic LHNs consist of both LH local neurons (LHLNs) and LH output neurons (LHONs). Uniglomerular projection neurons (uPNs) (green) provide the major excitatory input to glutamatergic LHNs (yellow) while they also receive feedback input (either excitation or inhibition) from LHLNs (**Bates et al., 2020**). LHLNs have been reported to inhibit each other as well as LHONs as well (**Bates et al., 2020**). LHONs, in addition to providing feedback excitation to LHLNs, relay the information to further higher brain centers. mPNs provide an odorant-selective inhibition to glutamatergic LHNs. mPNs are known to encode odor valence in the LH (**Strutz et al., 2014**),

Figure 6 continued on next page

Figure 6 continued

uPNs and glutamatergic LHNs encode odor identity as well as odor valence. The thickness of the line indicates the strength of excitatory or inhibitory input. The table illustrates that uPNs encode an improved odor identity than postsynaptic glutamatergic LHNs, whereas hedonic valence is equally maintained at the level of uPNs and glutamatergic LHNs in the LH.